

Article

Unravelling Microbial Communities Associated with Different Light Non-Aqueous Phase Liquid Types Undergoing Natural Source Zone Depletion Processes at a Legacy Petroleum Site

Melanie C. Bruckberger ^{1,2,*}, Deirdre B. Gleeson ², Trevor P. Bastow ¹, Matthew J. Morgan ³, Tom Walsh ³, John L. Rayner ¹, Greg B. Davis ¹ and Geoffrey J. Puzon ¹

¹ Centre for Environment and Life Sciences, CSIRO Land and Water, Private Bag No 5, Wembley, WA 6913, Australia; Trevor.Bastow@csiro.au (T.P.B.); John.Rayner@csiro.au (J.L.R.); Greg.Davis@csiro.au (G.B.D.); Geoffrey.Puzon@csiro.au (G.J.P.)

² UWA School of Agriculture and Environment, University of Western Australia, 35 Stirling Hwy, Crawley, WA 6009, Australia; deirdre.gleeson@uwa.edu.au

³ Black Mountain Laboratories, CSIRO Land and Water, Acton, P.O. Box 1700, Canberra, ACT 2601, Australia; Matthew.Morgan@csiro.au (M.J.M.); Tom.Walsh@csiro.au (T.W.)

* Correspondence: m.bruckberger@outlook.com



Citation: Bruckberger, M.C.; Gleeson, D.B.; Bastow, T.P.; Morgan, M.J.; Walsh, T.; Rayner, J.L.; Davis, G.B.; Puzon, G.J. Unravelling Microbial Communities Associated with Different Light Non-Aqueous Phase Liquid Types Undergoing Natural Source Zone Depletion Processes at a Legacy Petroleum Site. *Water* **2021**, *13*, 898. <https://doi.org/10.3390/w13070898>

Academic Editor: Stefano Polesello

Received: 28 February 2021

Accepted: 15 March 2021

Published: 25 March 2021

Publisher's Note: MDPI stays neutral with regard to jurisdictional claims in published maps and institutional affiliations.



Copyright: © 2021 by the authors. Licensee MDPI, Basel, Switzerland. This article is an open access article distributed under the terms and conditions of the Creative Commons Attribution (CC BY) license (<https://creativecommons.org/licenses/by/4.0/>).

Abstract: Petroleum contaminants are exposed to weathering when released into environment, resulting in the alteration of their chemical composition. Here, we investigated microbial communities through the soil profile at an industrial site, which was exposed to various petroleum products for over 50 years. The petroleum is present as light non-aqueous phase liquid (LNAPL) and is undergoing natural source zone depletion (NSZD). Microbial community composition was compared to the contaminant type, concentration, and its depth of obtained soil cores. A large population of Archaea, particularly *Methanomicrobia* and *Methanobacteria* and indication of complex syntrophic relationships of methanogens, methanotrophs and bacteria were found in the contaminated cores. Different families were enriched across the LNAPL types. Results indicate methanogenic or anoxic conditions in the deeper and highly contaminated sections of the soil cores investigated. The contaminant was highly weathered, likely resulting in the formation of recalcitrant polar compounds. This research provides insight into the microorganisms fundamentally associated with LNAPL, throughout a soil depth profile above and below the water table, undergoing NSZD processes at a legacy petroleum site. It advances the potential for integration of microbial community effects on bioremediation and in response to physicochemical partitioning of LNAPL components from different petroleum types.

Keywords: biodegradation; weathered; petroleum; microbial community; LNAPL; NSZD

1. Introduction

Long-term exposure of hydrocarbon derived contaminants is widely understood to adversely impact environmental ecosystems [1,2]. Hydrocarbon contaminants, such as crude oil, consist of a large number of components that can be altered through abiotic and biotic weathering processes after release into the environment [3]. Weathering can change the chemical composition of hydrocarbon-derived contaminants and is influenced by a range of factors, including soil properties and the indigenous microbial community [4]. Contaminated soil communities are typically enriched for microorganisms that are able to utilize a wide variety of hydrocarbons as food and energy sources [5,6]. The microbial community composition further depends on factors like predominant environmental conditions, for example, available electron acceptors and the extent of biodegradation and the composition of the petroleum [7,8]. Biodegradation in aerobic conditions results in the most efficient and complete mineralization of hydrocarbon-derived contaminants [9], however, oxygen is commonly found to be depleted in highly contaminated sites [10,11]. Biodegradation under anaerobic conditions is well-researched, however, it is known to

be less efficient [12]. In addition to less favorable electron acceptors being utilized, biodegraded contaminants comprising mainly of an unresolved complex mixture (UCM) are often found at legacy spills [13,14]. Polar compounds are reported to form from the partial oxidation of hydrocarbons and to accumulate in highly weathered diesel [15]. These represent a large complex group of unidentified oxygen containing compounds, likely formed through biodegradation processes that accumulated due to their recalcitrant nature [7,15]. Physicochemical processes such as dissolution and volatilization of components of the petroleum fuels can also lead to significant compositional changes [16]. Such changes likely alter the biodegradability of the remaining petroleum contaminant and the associated microbiological communities.

An industrial site located 50 km south of Perth, Western Australia, was exposed to different petroleum contaminants, including weathered hydrocarbons possibly > 50 years in age [17]. The contaminants at the site (including jet fuel/kerosene, diesel, and crude oil range products), affected by natural source zone depletion (NSZD), are present in the subsurface as a light non-aqueous phase liquid (LNAPL). The magnitude of NSZD processes [18,19] can be used as benchmark and is of significance for comparison to the effectiveness and need for implementation of different engineered remediation methods [20]. Previous investigations at the site showed the presence of a highly weathered diesel that could be >50 years in age [17]. Different potential remediation methods were investigated at the site, including air sparging of dissolved petroleum hydrocarbons [21], and air sparging in combination with soil vapor extraction on gasoline NAPL [22]. In addition, Multiphase Extraction [23] and biosparging [24] were explored. Further, biodegradation rates of spilled gasoline at the site were investigated, showing the consideration of structures in layered sandy vadose zones to be essential, in order to obtain accurate estimations [25]. While the majority of the previous studies at the site investigated the compositional changes to the hydrocarbons resulting from biodegradation, limited research targeted the microbiology of the contaminated soil and aquifer. Previous studies attempted to gain microbial insights using fatty acid methyl esters (FAME) derived signatures [26], and radiometric hydrocarbon mineralization [27]. However, FAME analysis is limited in its capacity to identify microbial taxa, and DNA-based techniques are more likely to provide better resolution and understanding of the microbial community associated with the NSZD at an LNAPL contaminated legacy site. The similar environmental characteristics across the site and exposure to individual petroleum-derived contaminants at different sections, make this a unique opportunity to directly compare the microbial communities established at different depths and contaminant concentrations, after significant weathering. This knowledge adds to the understanding of LNAPL undergoing NSZD, which can support effective management of similar sites. A recent microcosm study gave first indications of bacterial taxa, possibly associated with polar compounds, by using amplicon sequencing [7]. The microcosm study used polar compounds extracted from the weathered diesel present at the site, and compared the bacterial families established after 2 and 4 months under different conditions, to microcosms containing fresh diesel. While this microcosm study was able to identify changes of the microbial community, changes in response to the exposure to polar compounds and insights on the community established at the field sites are yet to be explored [7]. Microbial communities depend on environmental properties present at the site, and can vary greatly with soil depth, water table fluctuations, nutrient- and oxygen availability, soil structure, and other factors. Changes of the microbial community composition with depth was shown in previous studies. For example, shallow soil samples obtained from a fallow field with a maximum depth of 120 cm, showed soil enzymes and carbon concentrations to decline with depth, and metagenomic analysis revealed strong patterns of bacterial taxa with depth [28]. Similar results were found in a study using phospholipid fatty acid analysis (PFLA) in soil samples up to 2-m deep [29], and in up to 12.74-m deep polycyclic aromatic hydrocarbons (PAH) contaminated soil cores, using denaturing gradient gel electrophoresis (DGGE) fingerprinting [30]. Changes of microbial

communities are commonly explained by variations in resource availability with depth, such as total organic carbon (TOC) and carbon as a food source [31].

While gasoline and diesel contaminants and their potential remediation at the legacy site in Western Australia has been the main research focus in the past [17,21,22,25], this study presented the first detailed analysis of the microbial communities at this legacy site in Western Australia. The method used was 16S rRNA metabarcoding, which identified potential degradation scenarios at different locations of the site contaminated with three petroleum products (jet fuel/kerosene, diesel, and crude oil range products). In addition, it investigated microorganisms within and associated with the LNAPL itself, and not just the dissolved or volatile phases. The three LNAPL types consisted of many different components and carbon ranges, depending on their original source and how they were processed. For biodegradation to readily occur, different compounds required different metabolic pathways and enzymes produced by indigenous microorganisms, which resulted in the enrichment of different taxa associated with different LNAPL types [32]. Here we report insights into the microorganisms present with depth and with changing contaminant concentrations and conditions, by investigating multiple soil cores recovered across the depth of LNAPL contamination that lay above and below the notional water table at the site. This provided new insights into the differences and conditions dominating different sub-surface sections, influencing not only the microbial communities but also the contaminant characteristics. This was compared to uncontaminated control cores. LNAPL samples were also recovered from the existing wells. The research here provides novel insights into the microbial communities established in the LNAPL zone, undergoing active NSZD. The results of this study support integrated and long-term assessment of the effectiveness and persistence of the biodegradation processes for petroleum hydrocarbons, where engineered intervention might no longer be practicable [19]. The investigated site has a long history of different hydrocarbon spills, which were exposed to the environment for extended periods of time. Because environmental characteristics across this site are homogenous, the weathering of the individual compounds and the associated microbial communities established could be directly compared. Of particular importance, and the main focus of the current work, are polar compounds, which are known to accumulate at legacy spills, but are poorly characterized in the literature. The presence and recalcitrance of the polar compounds (from weathered diesel) found at this specific site was previously shown in a microcosm study [7], which also suggested the enrichment of specific other bacterial families (including *Kordiimonadaceae*, *Hyphomicrobiaceae*, and *Kiloniellaceae*) as compared to fresh diesel spills [7].

We hypothesize that the weathering extent likely differed between the contaminants, as well as with depth, resulting in the enrichment and abundance of specific hydrocarbon degrading microorganisms. The extent of biodegradation and the presence of polar compounds formed from weathering of different hydrocarbon precursors, was expected to have led to the formation of different microbial communities, enriching specific degraders. This study identified the differences in microbial communities established under different weathered petroleum contaminants, when exposed to similar environmental conditions, and suggests potential microbial degraders that might be able to utilize contaminants with a high polar compound content as a food source.

The current work follows, but more specifically builds on, a significant body of previous research conducted at this site and adds significantly to our understanding of the processes and difficulties commonly encountered at legacy spill sites, which have a significant impact worldwide.

2. Materials and Methods

2.1. Site Description and Soil Coring

Soil samples were collected from an industrial site with a long history of hydrocarbon contamination (>50 years). The site was located 50 km south of Perth, on the Swan Coastal Plain [33], and lay adjacent to the ocean. It was described as part of the Quindalup Dune

system [34] and the predominant geology at the site was known as Safety Bay Sands [35], consisting mainly of aeolian and littoral calcareous sand. Releases of hydrocarbons over several years including jet fuel/kerosene, diesel, and crude oil led to contamination of the subsurface soil and the aquifer, resulting in both mobile and immobile LNAPLs.

Samples were obtained from the site in September 2016. At the site, 4 locations representing 3 LNAPL types (jet fuel, diesel, and crude oil range products) and an uncontaminated background site were investigated. Two cores were obtained for the uncontaminated background, jet fuel and diesel range products; while three cores were obtained for crude oil range product (9 cores in total) (Table 1). The soil profile was predominantly leached sand with low organic carbon (<0.03%), with some limestone nodules, as previously described [25]. Soil cores were obtained by drilling, using a Geoprobe 6620 drilling rig with a Geoprobe dual tube 37 system, combined with a dual tube 32 internal sample system. Nine locations were selected for coring at depths of 1.50 m below ground level (bgl) to a maximum depth of 5.10 m bgl. The cores were then vertically cut into 0.05 m long sections, placed in sterile, sealed tins and transported on ice. Soil cores were subsampled for chemical analyses, and microbiome investigations and soil samples were stored in $-80\text{ }^{\circ}\text{C}$ freezers, prior to DNA extraction. Representative sections of each soil core were selected, to allow a comparison of similar conditions across the cores and contaminants. Sections were chosen to represent defined categories and included: 'Top' (T), to capture the top of the core near the surface (average 2.28 m); 'potential Water Table' (WT), capturing the likely water table interface (average 3.05 m), 'Mid' (M), likely the highest contaminated area (average 3.78 m), and 'Bottom' (B), capturing the deepest contaminated region (average 4.48 m).

Table 1. Depth profile and TPH concentrations (g/kg) of the selected sections of the investigated soil cores including—Top (T), Water table (WT), Mid (M), and Bottom (B). Two cores each of the background, jet fuel, and diesel sites; and three cores of the crude oil contaminated site were analyzed.

Section *		Core 1		Core 2		Core 3	
		Depth [m]	TPH [g/kg]	Depth [m]	TPH [g/kg]	Depth [m]	TPH [g/kg]
Background	T	2.00–2.05	0.0	2.00–2.05	0.0		
	WT	2.65–2.70	0.0	2.60–2.65	0.0		
	M	3.35–3.40	0.0	3.90–3.95	0.0		
	B	4.00–4.05	0.0	5.00–5.05	0.0		
Jet fuel	T	1.50–1.55	0.0	2.60–2.65	0.0		
	WT	2.20–2.25	0.9	3.35–3.40	16.4		
	M	3.35–3.40	25.0	3.80–3.85	22		
	B	4.00–4.05	4.9	4.15–4.20	1.3		
Diesel	T	3.00–3.05	0.0	2.95–3.00	0.0		
	WT	3.75–3.80	0.0	3.85–3.90	50.9		
	M	4.15–4.2	92.7	3.90–3.95	155.7		
	B	5.05–5.10	0.0	4.60–4.67	9.2		
Crude oil	T	2.65–2.70	13.2	3.00–3.05	0.0	0.0	2.95–3.00
	WT	3.10–3.15	25.3	3.70–3.75	21.1	0.0	3.10–3.15
	M	3.30–3.35	45.6	3.80–3.85	56.4	55.9	3.35–3.40
	B	3.90–3.95	1.6	4.05–4.10	2.3	0.0	3.90–3.95

* Vertical location of triplicate samples collected from site.

Soil liquid contents, were determined gravimetrically by oven drying at $105\text{ }^{\circ}\text{C}$ for 24 h. Samples were allowed to air dry prior to being placed in the oven, to remove the majority of volatile components.

2.2. Chemical Analysis

2.2.1. Extraction of Soil Core Samples

Soil cores were subsampled and 3–5 g was extracted using 4 mL of dichloromethane (DCM), which contained deuterated internal standards (d6-benzene, d8-toluene, d10-p-

xylylene, d8-naphthalene, d14-p-terphenyl). Soil samples were extracted using the tumbling method and sonication. After removal of the extraction solvent, extracts were placed into 5 mL vials (as well as DCM washings), providing samples ready for analysis by gas chromatography–flame ionizing detector (GC–FID) and gas chromatography–mass spectrometry (GC–MS).

2.2.2. GC–FID and GC–MS Analysis of Soil Core Samples

GC–FID analysis of total petroleum hydrocarbon (TPH) was performed using an Agilent 6890 GC fitted with a vaporizing injector (320 °C and operating in split mode), an auto-sampler, a flame ionizing detector (FID, held at 330 °C) and using helium as a carrier gas (1 mL min^{−1} flow). The GC–FID was fitted with a capillary GC column (Phenomenex ZB—1 ms, 30 m length, 0.25 mm internal diameter and 0.25 µm thick film of dimethyl polysiloxane or equivalent column). The oven temperature program was initially held at 35 °C for 1 min and then ramped at 15 °C/min to 330 °C and held at isothermal for 10 min. Quantitation of the total petroleum hydrocarbon (TPH) was performed using external standards containing the same internal standards for the samples.

GC–MS analysis of core samples was performed using an Agilent 7890 GC fitted with a vaporizing injector (320 °C operating in split mode, helium as carrier gas (1 mL min^{−1} flow)), an auto-sampler, and an Agilent 7000B mass spectrometer. The GC–MS was fitted with a capillary GC column (Phenomenex ZB—1 ms, 30 m length, 0.25 mm internal diameter, and 0.25 µm thick film of dimethyl polysiloxane or equivalent column). The oven temperature program was initially held at 35 °C for 3 min and then ramped at 15 °C/min to 330 °C and held at isothermal for 10 min. The mass spectrometer was operated with an ionization energy of 70 eV at 230 °C in the scan mode. Components in the samples were identified, based on known retention times and mass spectra characteristics. Quantitation of selected analytes was performed using external standards containing the same internal standards used for the samples.

2.2.3. LNAPL Sampling

LNAPL was also directly sampled from wells for analysis. Sampling was conducted by lowering a 40 mL VOA vial on a nylon dishing line directly into the well, just below the fluid (LNAPL) interface. The vial was retrieved, sealed, and transported to CSIRO for further processing. LNAPL samples were analyzed by GC–FID and GC–MS.

2.2.4. GC–FID and GC–MS Analysis of LNAPL Samples

LNAPL samples were directly analyzed (without dilution in solvent) using GC–FID on a HP 6890 GC. The GC was fitted with an autosampler, a vaporizing injector (320 °C operating in split mode), a flame ionizing detector (FID, held at 330 °C), and helium carrier gas (1 mL min^{−1} flow). A column with a 60 m × 0.25 mm diameter, coated with a 0.25-µm thick film of dimethyl polysiloxane (DB-1 UI, J&W) was used. The oven temperature program was initially held at 35 °C for 3 min and then ramped at 10 °C/min to 330 °C and held isothermal for 20 min. Components in the samples were identified, based on known retention times and mass spectra characteristics.

GC–MS analysis of LNAPL samples (diluted in dichloromethane) was performed using an Agilent 7890 GC fitted with a vaporizing injector (320 °C operating in splitless mode, helium as carrier gas (1 mL min^{−1} flow)), an auto-sampler, and an Agilent 7000B mass spectrometer. The GC–MS was fitted with a capillary GC column (J&W DB-1 UI, 60-m length, 0.25-mm internal diameter, and 0.25-µm thick film of dimethyl polysiloxane or an equivalent column). The oven temperature program was initially held at 35 °C for 3 min and then ramped at 10 °C/min to 330 °C and held isothermal for 20 min. The mass spectrometer was operated with an ionization energy of 70 eV at 230 °C in scan mode. Components in the samples were identified, based on known retention times and mass spectra characteristics.

2.3. Microbial Community Analysis

For each core, DNA was extracted from the selected core sections in triplicates (Table 1). The sections were selected by the position of the water table, as well as TPH concentrations. The four sample selections were from the following locations—(1) above (T) and (2) at the water table (WT), (3) below the water table with high TPH concentrations (M), and (4) a sample near the bottom of the contaminated zone (B), with lower contaminant concentrations. DNA was extracted from the selected soil core sections in triplicate (0.5 g of soil), using the PowerBiofilm DNA Isolation Kit (MoBio Laboratories, Inc., Carlsbad, CA, USA), following the manufacturer's instructions. Extracted DNA replicate was quantified on a Qubit fluorometer (Invitrogen) and stored at -80°C , prior to further processing. Microbiome analysis results are presented as one sample (combination of the three replicate sequencing datasets) per soil core section.

DNA extracts were processed as previously described [8], in brief, 16S rRNA Illumina sequencing (2 stage Illumina amplicon protocol) was performed on the DNA extracts, using the primers 515f (5'-GTGCCAGCMGCCGCGGTAA-3') and 806rcbc (5'-GGACTACHVGGGTWTCTAAT-3') for the PCR step. The PCR product was cleaned up using SPRI beads (Ampure XP beads, Beckman Coulter, Brea, California, USA), and the process was repeated. Sequencing was performed on an Illumina MiSeq (v3 600 bp), following the manufacturer's protocol (Illumina, San Diego, California, USA). Raw 16S files from the DNA sequencing were processed using QIIME v1.9.1 [36], based on a published workflow [37]. Paired-ends were stitched together using PEAR (v0.9.10) [38] and quality was confirmed by FastQC. Reads with a lower quality score of 28 and minimum of 90% of bases passing the quality cut-off, were then filtered using the `read_filter.pl` command, using the FASTX-Toolkit (v 0.7) and BBmap (v 35.84). Reads below 250 bp length were also removed [39,40]. Ambiguous bases in the filtered reads were removed by the `run_fastq_to_fasta.pl` command. Chimeric reads were removed by `chimera_filter.pl`, which uses VSEARCH and implements the uchime algorithm [41,42]. The RDP taxonomic database was used [43]. The files were combined into a single fasta file by `add_qiime_labels.py`, and then open reference OTU picking was performed using `uclust` [42] with a minimum specified OTU size of 1 to be included. OTUs identified in fewer than 0.1% of the reads were filtered out and the reads were rarefied to a minimum of 3700 in the samples. QIIME output was analyzed in a similar way, as described previously [44], using R v3.3.2 [45]. The OTU table was aggregated (L5 level), visualized as heatmaps using the `ggplot2` [46], and data were further processed using the `vegan` package [47]. Alpha diversity was calculated based on numbers of OTUs and Faith's phylogenetic diversity (Faith's PD), and visualized using `ggplot2` [46]. Beta-diversity patterns were shown as described before [44], with the Bray Curtis dissimilarity and nonmetric multidimensional scaling (NMDS), using the `metaMDS` function in the `vegan` package [47]. Taxa and selected subsurface environmental parameters (TPH, Depth, Moisture) with significant correlation to the species abundance in the samples were calculated with the `bio.env` function [48] and plotted on the ordination described above. Pairwise comparisons between levels of factors were implemented using the `adonis` function [47]. Further, PERMANOVA for multivariate null hypotheses of no difference among different groups and variance partitioning was analyzed, using the `Adonis` function of the `vegan` package [47] in R v3.3.2 [45].

3. Results

3.1. Chemical Analysis

Soil core samples contaminated with jet fuel/kerosene, diesel, and crude oil, were analyzed for their contaminant concentration (TPH, Table 1), using GC-FID. Generally, the highest TPH concentrations were measured in the M sections of the cores, which ranged from 0.9 mg/kg (jet fuel/kerosene) to a maximum of 155 mg/kg (diesel) (Table 1). Most T sections of the cores had no detectable TPH, except the crude oil core which had 13.2 mg/kg TPH. No detectable TPH concentration was measured in the uncontaminated background cores.

The core samples and LNAPL from areas associated with the contaminated cores were investigated and their composition was assessed. The cores with diesel range product showed a TPH with a limited carbon range of C₉–C₂₈, and signs of weathering, as suggested by the absence of *n*-alkanes and the altered distribution of methylalkanes and isoprenoids (Figure 1A). The LNAPL associated with of the jet fuel/kerosene range product (predominately C₇–C₁₆ components) also showed signs of weathering with the depletion of *n*-alkanes and the presence of tetraalkylleads (TALs, identified using GC–MS analysis), indicating remnants of leaded gasoline product in the sample. The depletion of *n*-alkanes was likely due to biodegradation, while lower molecular weight compounds and water soluble components (such as benzene, toluene, ethylbenzene, and xylene—the BTEX) were likely depleted by volatilization and dissolution (Figure 1B). The TPH signature of the core samples associated with the jet fuel/kerosene range product appeared to be altered with depth through biodegradation, with the relative depletion of some aromatic components (BTX and trimethylbenzenes) with depth. The crude oil contaminated soil cores had TPH with a carbon range of C₇–C₄₀, which was a broader range than that usually observed in single fuel types, and signs of weathering were observed (Figure 1C). Additionally, the TPH was more biodegraded in shallower samples with the depletion of less recalcitrant isoprenoids (pristane) (depleted relative to norpristane and phytane). The changes in the TPH composition indicated different subsurface conditions with deeper core samples that were less affected by biodegradation and were likely due to more aerobic conditions impacting shallower samples.

3.2. Microbial Community Analysis

Alpha diversity across all cores investigated in this study showed variations between the core sections. Uncontaminated background cores showed the highest Faith's PD values in the WT sections, and the lowest values in the B sections. Alpha diversity varied between sections of the soil cores exposed to contaminants and shared no similar trend (Supplementary Figures S1–S4).

Beta diversity patterns visualized in the NMDS ordination plot, showed significant correlation with the environmental parameters 'Depth' and 'TPH', when testing different factors (TPH, Depths, Moisture, and Section of the core) (Figure 2). Samples mainly impacted by these factors included the WT, M, and B sections of diesel or crude oil exposed soil cores. Samples from the B section of the diesel-, and some crude oil cores showed correlations with members belonging to *Methanobacteriaceae*, *Methanosaetaceae*, *Anaerolinaceae*, and *Syntrophaceae* when fitted onto ordination. Additionally, an enrichment of *Methanoregulaceae* and *Methanocellaceae*, along with bacterial families *Syntrophaceae*, *Syntrophorhabdaceae*, and *Syntrophobacteriaceae* was observed in the WT, M, and B sections of the diesel-contaminated cores. The T section showed increased abundance of members belonging to *Thaumarchaeota* (Figure 3). Similar to the diesel-contaminated samples, archaeal families were identified in the WT, M, and B sections of crude-oil-exposed soil (Figure 4). An additional high abundance of NRA6_Unknown (*Methanomicrobia*) and *Methanomassiliicoccaceae* were found in the crude oil samples. Unclassified bacteria OP8 (clone OPB95) and *Syntrophaceae* were also enriched (Figure 4). In the WT, M, and B sections of the jet-fuel-contaminated cores, similar archaeal families were identified, as compared to crude oil and diesel samples. Additionally, an increased presence of some *Alphaproteobacteria* including members of *Rhodospirillaceae* and *Xanthobacteriaceae* was noted (Figure 5). Jet-fuel-contaminated samples were not significantly correlated with TPH and Depth when fitted onto ordination, but the M and B sections showed correlation with bacterial families, including *Hyphomicrobiaceae*, *Comamonadaceae*, and *Porphyromonadaceae* (Figure 2). Samples from the uncontaminated background cores showed a similar 16S rRNA beta diversity across all sections and were correlated with members of common soil organisms, such as AK32 (*Thaumarchaeota*), *Syntrophobacteriaceae*, *Methanomassiliicoccaceae*, and members of *Nitrospirales* (Figure 2). High abundance of MBGA and members belonging to *Thaumarchaeota* were found across all

sections of the background cores, while MCG, *Nitrospira*, and *Brocardiaceae* was enriched in the M and B sections (Supplementary Figure S5).

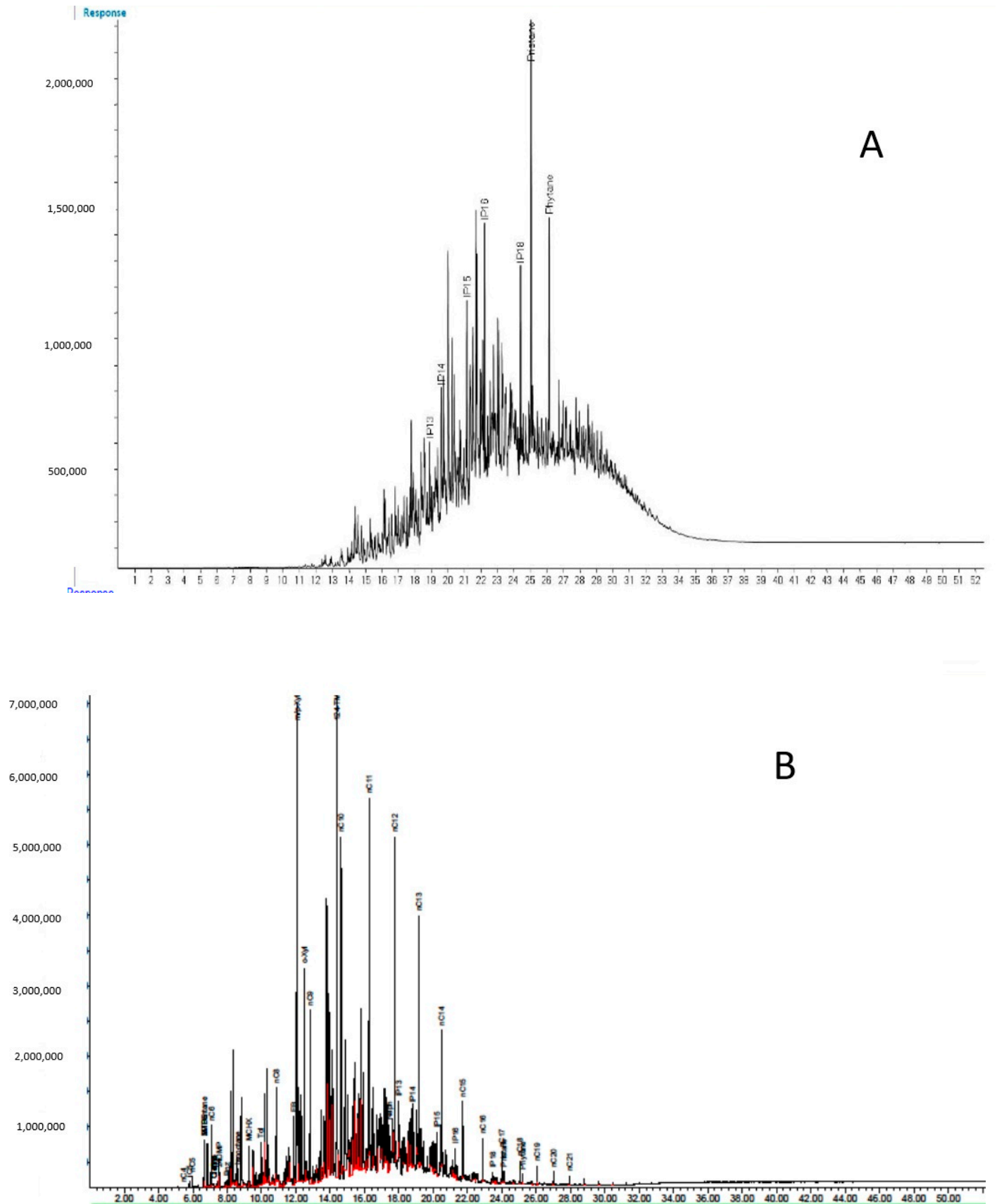


Figure 1. Cont.

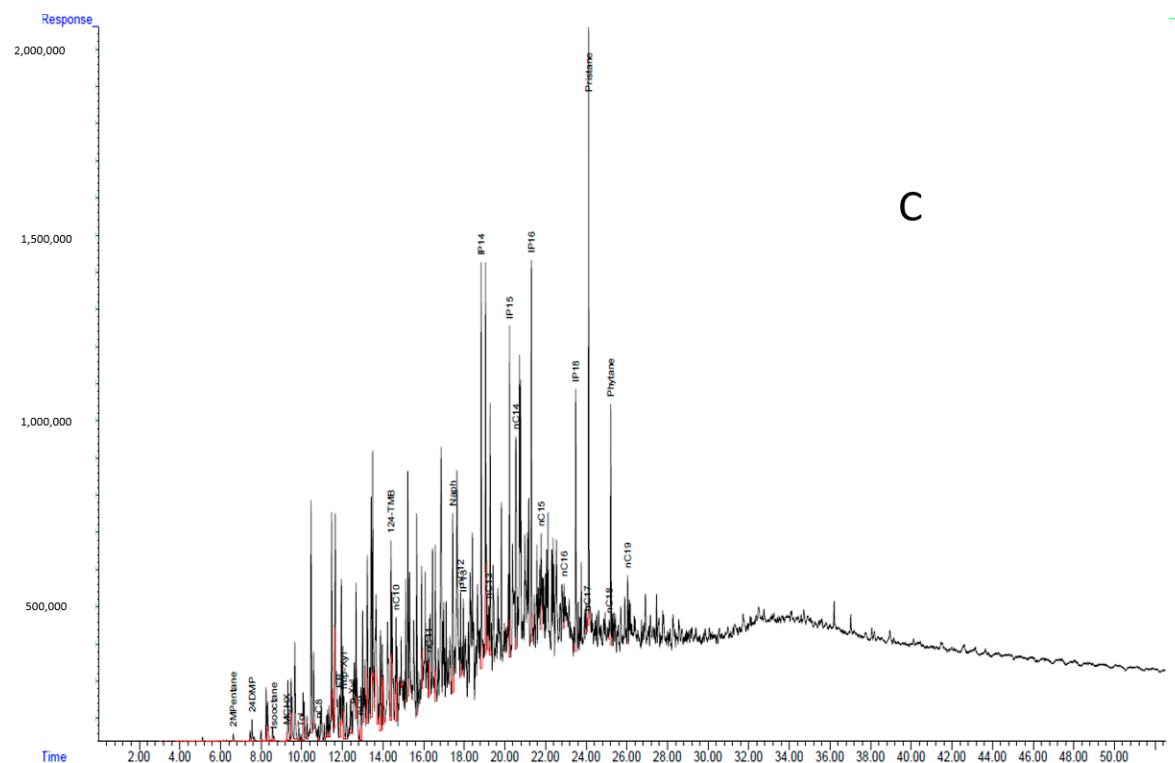


Figure 1. GC–FID analysis of the obtained LNAPL samples. Analysis of diesel- (A), jet-fuel- (B), and crude-oil- (C) contaminated cores. CHX—cyclohexane, Cs—straight or branched alkane containing x carbons, EB—ethylbenzene, IP— isoprenoid, Tol—toluene, and Xyl—xylene.

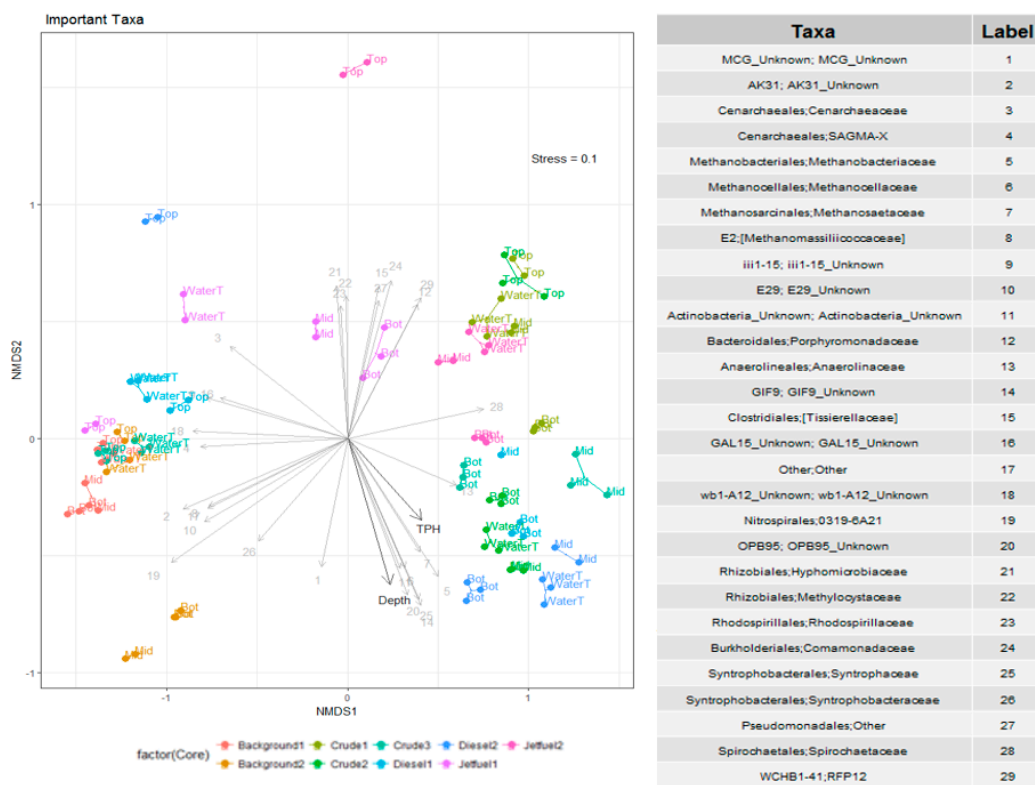


Figure 2. Significant environmental parameters and abundant taxa. Non-metric multidimensional scaling (NMDS) plot based on the Bray Curtis dissimilarity. Vectors show the most abundant taxa present (>4% relative abundance) and environmental parameters determined to be significant.

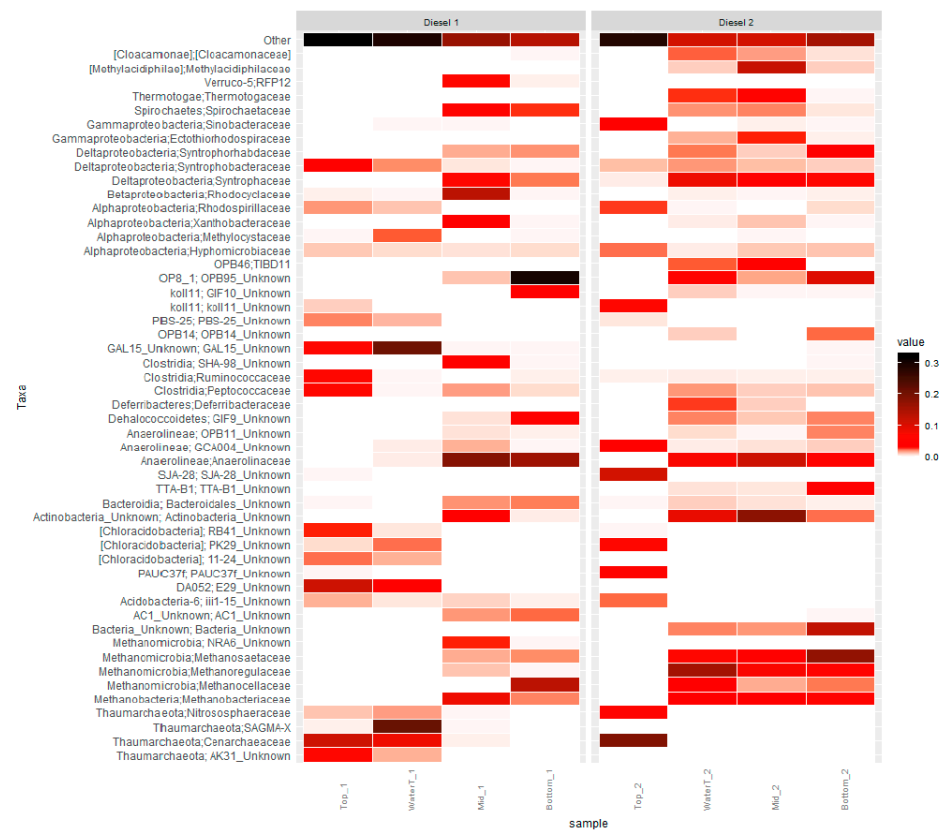


Figure 3. Most abundant taxa in diesel-contaminated cores. Heatmap of the most abundant (>2%) taxa in the diesel-contaminated cores, based on next generation sequencing of 16S rRNA genes.



Figure 4. Most abundant taxa in crude-oil-contaminated cores. Heatmap of the most abundant (>2%) taxa in the crude-oil-contaminated cores, based on next generation sequencing of 16S rRNA genes.

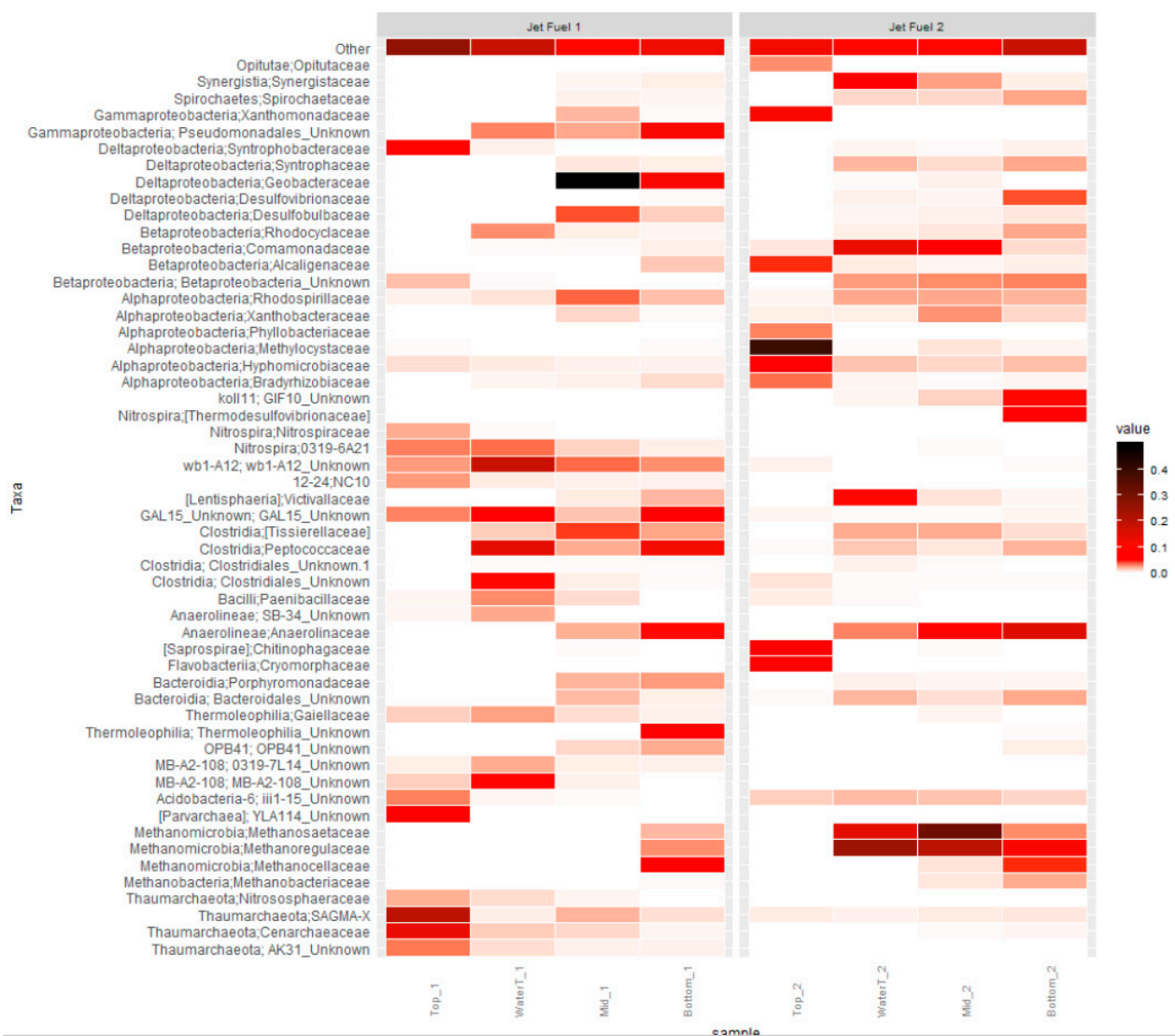


Figure 5. Most abundant taxa in jet-fuel-contaminated cores. Heatmap of the most abundant (>2%) taxa in the jet-fuel-contaminated cores, based on next generation sequencing of 16S rRNA genes.

Samples were further inspected for significant effects of contaminant type, TPH, and depth by PERMANOVA (Supplementary Table S1). Results indicated that contaminant type had a significant effect ($p < 0.015$), which explained 13% of the variance in the microbial community structure. The pairwise PERMANOVA comparison showed a significant difference between the community structure found in the background cores and the contaminated cores. Additionally, a significant difference ($p < 0.02$) was detected between jet-fuel- and diesel-exposed communities (Supplementary Table S1).

4. Discussion

This study investigated microbial communities in soil cores obtained from a contaminated legacy site in Western Australia, where NSZD of the three contaminant LNAPL types occur. While the area of the industrial site shares similar environmental characteristics, individual sections were exposed to different hydrocarbon contaminants over a long period of time. This offers the opportunity for a direct comparison of weathering processes and enriched microorganisms across different contaminants. Interestingly, the microbial communities established in soil cores exposed to the LNAPL contaminants and the uncontaminated background cores, showed a high abundance of archaeal families. While the most dominant archaea in the background cores belonged to common soil archaea such

as *Thaumarchaeota*, MCG, and MBGA, contaminated cores showed high abundances of archaea belonging to classes *Methanomicrobia* and *Methanobacteria*. Similar archaeal classes were found across the cores, but on a family level, diesel, jet fuel, and crude oil appear to have enriched different members. Known methanogens were predominantly identified in the deeper sections of the cores where the highest LNAPL concentrations were measured, and anaerobic conditions likely dominated. This agreed with findings of a study conducted by Franzmann et al. (2002), where anoxic conditions were shown at the same site [49]. Interestingly, the past study identified sulfate as the main electron acceptor for toluene biodegradation, especially as no methane was detected in the plume. However, little evidence of sulfate reducing organisms was found using FISH and phospholipid fatty acid analysis, with *Desulfosporosinus meridie* being the only sulfate reducer isolated from the plume [49]. This might be a result of the previous methods used, which were not capable of identifying the detailed microbial diversity. In the present study, microorganisms were well-characterized in the contaminated soil cores, and several methanotrophs such as *Methylocystaceae* (T, WT) and *Methylacidiphilaceae* (WT, M, B) [50] were found in cores contaminated by diesel jet fuel/kerosene range products, as well as class Verruco-5 (T, WT, M, B) of phylum *Verrucomicrobia*, which is known to have methanotrophic members [51], that are also found in the crude oil cores. It is possible that the methane produced by methanogens is utilized by methanotrophs, explaining the conclusions of the past study. The presence of the identified methanogens in the deep sections, suggests a tolerance to or the ability to degrade the contaminants. For example, *Methanosaetaceae* and *Methanobacteriaceae*, enriched in the diesel and crude oil cores, were previously found as part of a deep-sea oil degrading community [52], and in methanogenic phenol degrading sludge [53], respectively. The most dominant member of the *Methanomicrobia* class in jet-fuel-contaminated soil cores, in addition to *Methanosaetaceae*, was *Methanoregulaceae*, which was shown to be enriched in methanogenic crude oil degrading cultures in a past study [54].

Core samples contaminated with jet fuel/kerosene range products showed a significantly different community structure, as compared to cores contaminated by diesel range products and background cores (Supplementary Table S1), and formed a separate cluster in the NMDS ordination (Figure 2), mainly driven by the significant correlation with the known degrading bacterial families *Hyphomicrobiaceae*, *Porphyromonadaceae*, *Xanthobacteriaceae*, and *Comamonadaceae*. The differences of the community enriched in the jet fuel/kerosene range product cores compared to diesel and crude oil, likely resulted from different contaminant compounds and concentrations being present. TPH analyses showed that in the jet fuel/kerosene product range, cores were differently affected by biodegradation, with depth, with loss of selected aromatic components (BTX, trimethylbenzenes with depth). These different subsurface conditions likely led to the biodegradation of different contaminant components, and therefore to the enrichment of specific microorganisms. Depending on their characteristics, hydrocarbon components can bind to soil particles, and differ in their bioavailability and biodegradability to microorganisms [55]. The bacterial families that significantly correlated with jet fuel cores (Figure 2) were previously also found at a hydrocarbon contaminated legacy site contaminated with polar compounds (metabolites, oxygen containing compounds) from the partial oxidation of hydrocarbons [8,44]. The high polar content previously identified in LNAPL samples obtained from the site in this study [15], and the high likelihood of similar compounds found in the weathered hydrocarbons present in this study, further strengthens the indication that these microorganisms have the ability to degrade or tolerate polar metabolites. Methanogenic conditions in the deep and contaminated sections of the cores, were further supported by an enrichment of bacterial families commonly found in syntrophic consortia with methanogens. For example, families found in diesel and crude oil cores included *Anaerolinaceae*, previously part of a methanogenic culture, after long-term (1300 days) alkane exposure, and *Syntrophaceae*, identified in weathered crude-oil-contaminated groundwater [44]. Diesel-contaminated cores also showed enrichment of *Syntrophorhabdaceae* in the deeper sections of the core, which is a known phenol degrader and is associated with hydrogen or acetate consuming

methanogens, and is occasionally found in sulfate reducing conditions [56,57]. The presence of *Peptococcaceae* in all three contaminant-exposed soil cores further suggests anaerobic and potentially methanogenic conditions, as it is a known anaerobic aromatic hydrocarbon degrader [58,59] that is found to exist in syntrophy with hydrogen utilizers [58–60].

Biodegradation of different hydrocarbon classes in the core samples with depth, suggested varying conditions with depth. GC–FID analysis of the LNAPL revealed signs of severe biotic and abiotic weathering in all three petroleum LNAPL types, likely containing polar metabolites [15], and was the cause of discoloration of recovered products from the site. The composition of the jet fuel/kerosene range product in the study showed depletion of the dominant C₇–C₁₆ components. The composition of the diesel displayed a limited carbon range (C₉–C₂₈), while crude oil comprised a broader range (C₇–C₄₀) that was consistent with it not being a refined petroleum product. All three contaminants revealed depletion or removal of *n*-alkanes, commonly observed in weathered petroleum [9,61], as it is one of the most readily biodegradable aliphatic compound classes, as shown in previous research [62]. Additional indications of weathering was the depletion of isoprenoids like pristane (relative to other isoprenoids such as phytane) in the diesel and crude samples (Figure 1A,C), similar to observations in another study [15]. Correlation analysis indicated depth and TPH as significant impacts on microbial community structure, however, it is difficult to determine which of the two factors are the main contributors of change (Figure 2). The different conditions in the soil cores likely resulted in different components preferentially being biodegraded and affecting the microbial community composition. Anaerobic or methanogenic conditions that appeared to be dominating might have resulted from initial biodegradation processes leading to oxygen depletion, commonly observed at legacy spills [44]. While biodegradation occurs under anaerobic conditions, it generally found to be slower and incomplete when compared to aerobic conditions [12].

The findings in this study identified the microbial communities associated with highly weathered petroleum (jet fuel/kerosene, diesel, and crude oil range products). Changes in the composition of the petroleum with depth, was possibly due to different compounds being preferentially degraded, which suggests methanogenic conditions with syntrophic and complex relationships. Several members were found in previous studies investigating weathered contaminants with a large polar content, indicating their association with those compounds. This study identified the dominant microbial community present during NSZD at an LNAPL-contaminated site, and transitions in the community due to composition, depth, and aerobic/anoxic status, along with the extent of weathering. This adds to the knowledge of the management of legacy spills, and the fate of highly weathered contaminants, and allows more reliable integration of processes governing NSZD at such contaminated sites.

Supplementary Materials: The following are available online at <https://www.mdpi.com/2073-4441/13/7/898/s1>. Figure S1 Community diversity in background cores. Alpha Diversity, calculated as Faith's Phylogenetic Diversity and by number of OTUs in the background cores, Figure S2 Community diversity in jet fuel contaminated cores. Alpha Diversity, calculated as Faith's Phylogenetic Diversity and by number of OTUs in the jet fuel contaminated cores., Figure S3 Community diversity in diesel contaminated cores. Alpha Diversity, calculated as Faith's Phylogenetic Diversity and by number of OTUs in the diesel contaminated cores, Figure S4 Community diversity in crude oil contaminated cores. Alpha Diversity, calculated as Faith's Phylogenetic Diversity and by number of OTUs in the crude oil contaminated cores., Figure S5 Most abundant taxa in background cores. Heatmap of the most abundant (>2%) taxa in the background cores, based on next generation sequencing of 16S rRNA genes, Table S1 PERMANOVA analysis and pairwise comparison.

Author Contributions: Writing—original draft preparation, microbial sample preparation and analysis, visualization, M.C.B.; writing—review and editing, methodology, D.G.; chemical analysis, writing—review and editing, T.P.B.; validation, methodology, M.M. and T.W.; sampling, J.L.R.; writing—review and editing, funding acquisition, G.B.D.; writing—review and editing, supervision, project administration, G.J.P. All authors have read and agreed to the published version of the manuscript.

Funding: This research received no external funding.

Institutional Review Board Statement: Not applicable.

Informed Consent Statement: Not applicable.

Data Availability Statement: Data has been published and access available at <https://data.csiro.au/collections/collection/CiCSiro:49662v1>, accessed on 15 January 2021.

Acknowledgments: The logistical support of BP, particularly David Donovan is gratefully acknowledged. Yasuko Geste is thanked for technical help with chemistry. Suzanne Metcalfe is thanked for her assistance with amplicon sequencing. David Beale and Yosephine Gumulya are thanked for valuable reviews and comments on the manuscript.

Conflicts of Interest: The authors declare no conflict of interest.

References

1. Sutton, N.B.; Maphosa, F.; Morillo, J.A.; Abu Al-Soud, W.; Langenhoff, A.A.M.; Grotenhuis, T.; Rijnaarts, H.H.M.; Smidt, H. Impact of Long-Term Diesel Contamination on Soil Microbial Community Structure. *Appl. Environ. Microbiol.* **2012**, *79*, 619–630. [[CrossRef](#)]
2. Aubé, J.; Senin, P.; Pringault, O.; Bonin, P.; Deflandre, B.; Bouchez, O.; Bru, N.; Biritxinaga-Etchart, E.; Klopp, C.; Guyoneaud, R.; et al. The impact of long-term hydrocarbon exposure on the structure, activity, and biogeochemical functioning of microbial mats. *Mar. Pollut. Bull.* **2016**, *111*, 115–125. [[CrossRef](#)]
3. Baek, K.H.; Kim, H.S.; Oh, H.M.; Yoon, B.D.; Kim, J.; Lee, I.S. Effects of crude oil, oil components, and bioremediation on plant growth. *J. Environ. Sci. Health Part A* **2004**, *39*, 2465–2472. [[CrossRef](#)]
4. Maletić, S.P.; Dalmacija, B.D.; Rončević, S.D.; Agbaba, J.R.; Perović, S.D.U. Impact of hydrocarbon type, concentration and weathering on its biodegradability in soil. *J. Environ. Sci. Health Part A* **2011**, *46*, 1042–1049. [[CrossRef](#)]
5. Atlas, R.M. Microbial degradation of petroleum hydrocarbons: An environmental perspective. *Microbiol. Rev.* **1981**, *45*, 180–209. [[CrossRef](#)]
6. Greene, E.A.; Kay, J.G.; Jaber, K.; Stehmeier, L.G.; Voordouw, G. Composition of Soil Microbial Communities Enriched on a Mixture of Aromatic Hydrocarbons. *Appl. Environ. Microbiol.* **2000**, *66*, 5282–5289. [[CrossRef](#)] [[PubMed](#)]
7. Bruckberger, M.C.; Bastow, T.P.; Morgan, M.J.; Gleeson, D.; Banning, N.; Davis, G.; Puzon, G.J. Biodegradability of polar compounds formed from weathered diesel. *Biodegradation* **2018**, *29*, 443–461. [[CrossRef](#)] [[PubMed](#)]
8. Bruckberger, M.C.; Morgan, M.J.; Walsh, T.; Bastow, T.P.; Prommer, H.; Mukhopadhyay, A.; Kaksonen, A.H.; Davis, G.; Puzon, G.J. Biodegradability of legacy crude oil contamination in Gulf War damaged groundwater wells in Northern Kuwait. *Biodegradation* **2019**, *30*, 71–85. [[CrossRef](#)] [[PubMed](#)]
9. Atlas, R.M.; Bartha, R. *Microbial Ecology: Fundamentals and Applications*; Addison-Wesley Publishing Company: Boston, MA, USA, 1981.
10. Fahy, A.; McGenity, T.J.; Timmis, K.N.; Ball, A.S. Heterogeneous aerobic benzene-degrading communities in oxygen-depleted groundwaters. *FEMS Microbiol. Ecol.* **2006**, *58*, 260–270. [[CrossRef](#)] [[PubMed](#)]
11. Davis, G.; Barber, C.; Power, T.; Thierrin, J.; Patterson, B.; Rayner, J.; Wu, Q. The variability and intrinsic remediation of a BTEX plume in anaerobic sulphate-rich groundwater. *J. Contam. Hydrol.* **1999**, *36*, 265–290. [[CrossRef](#)]
12. Ghattas, A.-K.; Fischer, F.; Wick, A.; Ternes, T.A. Anaerobic biodegradation of (emerging) organic contaminants in the aquatic environment. *Water Res.* **2017**, *116*, 268–295. [[CrossRef](#)]
13. Lundegard, P.D.; Knott, J.R. Polar organics in crude oil and their potential impacts on water quality. In Proceedings of the Petroleum Hydrocarbons and Organic Chemicals in the Ground Water NGWA/API Conference, Houston, TX, USA, 14–16 November 2001.
14. Lundegard, P.D.; Sweeney, R.E. Total Petroleum Hydrocarbons in Groundwater—Evaluation of Nondissolved and Nonhydrocarbon Fractions. *Environ. Forensics* **2004**, *5*, 85–95. [[CrossRef](#)]
15. Lang, D.A.; Bastow, T.P.; Van Aarssen, B.G.; Warton, B.; Davis, G.B.; Johnston, C.D. Polar Compounds from the Dissolution of Weathered Diesel. *Ground Water Monit. Remediat.* **2009**, *29*, 85–93. [[CrossRef](#)]
16. Lekmine, G.; Bastow, T.P.; Johnston, C.D.; Davis, G.B. Dissolution of multi-component LNAPL gasolines: The effects of weathering and composition. *J. Contam. Hydrol.* **2014**, *160*, 1–11. [[CrossRef](#)]
17. Johnston, C.D.; Bastow, T.P.; Innes, N.L. The use of biodegradation signatures and biomarkers to differentiate spills of petroleum hydrocarbon liquids in the subsurface and estimate natural mass loss. *Eur. J. Soil Biol.* **2007**, *43*, 328–334. [[CrossRef](#)]
18. Garg, S.; Newell, C.J.; Kulkarni, P.R.; King, D.C.; Adamson, D.T.; Renno, M.I.; Sale, T. Overview of Natural Source Zone Depletion: Processes, Controlling Factors, and Composition Change. *Ground Water Monit. Remediat.* **2017**, *37*, 62–81. [[CrossRef](#)]
19. Lari, K.S.; Davis, G.B.; Rayner, J.L.; Bastow, T.P.; Puzon, G.J. Natural source zone depletion of LNAPL: A critical review supporting modelling approaches. *Water Res.* **2019**, *157*, 630–646. [[CrossRef](#)] [[PubMed](#)]
20. Lari, K.S.; Rayner, J.L.; Davis, G.B. Towards characterizing LNAPL remediation endpoints. *J. Environ. Manag.* **2018**, *224*, 97–105. [[CrossRef](#)]

21. Johnston, C.; Rayner, J.; Patterson, B.; Davis, G. Volatilisation and biodegradation during air sparging of dissolved BTEX-contaminated groundwater. *J. Contam. Hydrol.* **1998**, *33*, 377–404. [[CrossRef](#)]
22. Johnston, C.; Rayner, J.; Briegel, D. Effectiveness of in situ air sparging for removing NAPL gasoline from a sandy aquifer near Perth, Western Australia. *J. Contam. Hydrol.* **2002**, *59*, 87–111. [[CrossRef](#)]
23. Johnston, C.; Fisher, S.; Rayner, J. *Removal of Petroleum Hydrocarbons from the Vadose Zone during Multi-Phase Extraction at a Contaminated Industrial Site*; IAHS PUBLICATION: Philadelphia, PA, USA, 2002; pp. 287–294.
24. Johnston, C.; Robertson, B.; Bastow, T. Evidence for the success of biosparging LNAPL diesel in the water table zone of a shallow sand aquifer. In *GQ07: Securing Groundwater Quality in Urban and Industrial Environments, Proceedings of the 6th International Groundwater Quality Conference, Fremantle, Australia, 2–7 December 2007*; International Association of Hydrological Sciences: Wallingford, UK, 2007.
25. Davis, G.B.; Rayner, J.L.; Trefry, M.G.; Fisher, S.J.; Patterson, B.M. Measurement and Modeling of Temporal Variations in Hydrocarbon Vapor Behavior in a Layered Soil Profile. *Vadose Zone J.* **2005**, *4*, 225–239. [[CrossRef](#)]
26. Franzmann, P.; Patterson, B.; Power, T.; Nichols, P.; Davis, G. Microbial biomass in a shallow, urban aquifer contaminated with aromatic hydrocarbons: Analysis by phospholipid fatty acid content and composition. *J. Appl. Bacteriol.* **1996**, *80*, 617–625. [[CrossRef](#)]
27. Franzmann, P.D.; Zappia, L.R.; Power, T.R.; Davis, G.B.; Patterson, B.M. Microbial mineralisation of benzene and characterisation of microbial biomass in soil above hydro-carbon-contaminated groundwater. *FEMS Microbiol. Ecol.* **1999**, *30*, 67–76. [[CrossRef](#)]
28. Ko, D.; Yoo, G.; Yun, S.-T.; Jun, S.-C.; Chung, H. Bacterial and fungal community composition across the soil depth profiles in a fallow field. *J. Ecol. Environ.* **2017**, *41*, 34. [[CrossRef](#)]
29. Fierer, N.; Schimel, J.P.; Holden, P. Variations in microbial community composition through two soil depth profiles. *Soil Biol. Biochem.* **2003**, *35*, 167–176. [[CrossRef](#)]
30. Ding, A.; Sun, Y.; Dou, J.; Cheng, L.; Jiang, L.; Zhang, D.; Zhao, X. Characterizing Microbial Activity and Diversity of Hydrocarbon-Contaminated Sites. *Hydrocarbon* **2013**, *18*. [[CrossRef](#)]
31. Zhou, J.; Xia, B.; Treves, D.S.; Wu, L.-Y.; Marsh, T.L.; O’Neill, R.V.; Palumbo, A.V.; Tiedje, J.M. Spatial and Resource Factors Influencing High Microbial Diversity in Soil. *Appl. Environ. Microbiol.* **2002**, *68*, 326–334. [[CrossRef](#)]
32. Das, N.; Chandran, P. Microbial Degradation of Petroleum Hydrocarbon Contaminants: An Overview. *Biotechnol. Res. Int.* **2011**, *2011*, 941810. [[CrossRef](#)]
33. Playford, P.E.; Low, G.; Cockbain, A.E. *Geology of the Perth Basin, Western Australia*; Geological Survey of Western Australia: Perth, Australia, 1976.
34. McArthur, W.M.; Bettenay, E. *The Development and Distribution of the Soils of the Swan Coastal Plain, Western Australia*; Soil Publication; CSIRO: Melbourne, Australia, 1960; p. 16.
35. Playford, P.E.; Low, G.H. Definitions of some new and revised rock units in the Perth Basin. *West. Aust. Geol. Surv. Annu. Rep.* **1971**, 44–46.
36. Caporaso, J.G.; Kuczynski, J.; Stombaugh, J.; Bittinger, K.; Bushman, F.D.; Costello, E.K.; Fierer, N.; Peña, A.G.; Goodrich, J.K.; Gordon, J.I.; et al. QIIME Allows Analysis of High-Throughput Community Sequencing data. *Nat. Methods* **2010**, *7*, 335–336. [[CrossRef](#)]
37. Comeau, A.M.; Douglas, G.M.; Langille, M.G.I. Microbiome Helper: A Custom and Streamlined Workflow for Microbiome Research. *mSystems* **2017**, *2*, e00127-16. [[CrossRef](#)] [[PubMed](#)]
38. Zhang, J.; Kobert, K.; Flouri, T.; Stamatakis, A. PEAR: A fast and accurate Illumina Paired-End reAd mergeR. *Bioinformatics* **2014**, *30*, 614–620. [[CrossRef](#)] [[PubMed](#)]
39. Bushnell, B. *BBMap: A Fast, Accurate, Splice-Aware Aligner*; Lawrence Berkeley National Lab (LBNL): Berkeley, CA, USA, 2014.
40. Gordon, A.; Hannon, G. Fastx-Toolkit. FASTQ/A Short-Reads Pre-Processing Tools. 2010. Available online: http://hannonlab.cshl.edu/fastx_toolkit (accessed on 20 January 2021).
41. Rognes, T.; Flouri, T.; Nichols, B.; Quince, C.; Mahé, F. VSEARCH: A versatile open source tool for metagenomics. *PeerJ* **2016**, *4*, e2584. [[CrossRef](#)]
42. Edgar, R.C. Search and clustering orders of magnitude faster than BLAST. *Bioinformatics* **2010**, *26*, 2460–2461. [[CrossRef](#)] [[PubMed](#)]
43. Cole, J.R.; Wang, Q.; Fish, J.A.; Chai, B.; McGarrell, D.M.; Sun, Y.; Brown, C.T.; Porras-Alfaro, A.; Kuske, C.R.; Tiedje, J.M. Ribosomal Database Project: Data and tools for high throughput rRNA analysis. *Nucleic Acids Res.* **2014**, *42*, D633–D642. [[CrossRef](#)]
44. Bruckberger, M.C.; Morgan, M.J.; Bastow, T.P.; Walsh, T.; Prommer, H.; Mukhopadhyay, A.; Kaksonen, A.H.; Davis, G.B.; Puzon, G.J. Investigation into the microbial communities and associated crude oil-contamination along a Gulf War impacted groundwater system in Kuwait. *Water Res.* **2020**, *170*, 115314. [[CrossRef](#)] [[PubMed](#)]
45. Team R Core. *R: A Language and Environment for Statistical Computing*; R Foundation for Statistical Computing: Vienna, Austria, 2014.
46. Wickham, H. *ggplot2: Elegant Graphics for Data Analysis*; Springer: Berlin/Heidelberg, Germany, 2016.
47. Oksanen, J. *Vegan: Community Ecology Package*. R Package Version 2.4–2. 2017. Available online: <https://mran.microsoft.com/snapshot/2017-02-04/web/packages/vegan/vegan.pdf> (accessed on 19 January 2021).
48. Taylor, M. *sinker: A Collection of Functions Featured on the Blog ‘me nugget’*. R Package Version 1.0. 2014. Available online: <https://github.com/menusugget/sinker> (accessed on 20 January 2021).

49. Franzmann, P.; Robertson, W.; Zappia, L.; Davis, G. The role of microbial populations in the containment of aromatic hydrocarbons in the subsurface. *Biodegradation* **2002**, *13*, 65–78. [[CrossRef](#)]
50. Lee, H.J.; Jeong, S.E.; Kim, P.J.; Madsen, E.L.; Jeon, C.O. High resolution depth distribution of Bacteria, Archaea, methanotrophs, and methanogens in the bulk and rhizosphere soils of a flooded rice paddy. *Front. Microbiol.* **2015**, *6*, 639. [[CrossRef](#)]
51. Sharp, C.E.; Smirnova, A.V.; Graham, J.M.; Stott, M.B.; Khadka, R.; Moore, T.R.; Grasby, S.E.; Strack, M.; Dunfield, P.F. Distribution and diversity of verrucomicrobia methanotrophs in geothermal and acidic environments. *Environ. Microbiol.* **2014**, *16*, 1867–1878. [[CrossRef](#)]
52. Campeão, M.E.; Reis, L.; Leomil, L.; De Oliveira, L.; Otsuki, K.; Gardinali, P.; Pelz, O.; Valle, R.; Thompson, F.L.; Thompson, C.C. The Deep-Sea Microbial Community from the Amazonian Basin Associated with Oil Degradation. *Front. Microbiol.* **2017**, *8*, 1019. [[CrossRef](#)]
53. Zhang, T.; Ke, S.Z.; Liu, Y.; Fang, H. Microbial characteristics of a methanogenic phenol-degrading sludge. *Water Sci. Technol.* **2005**, *52*, 73–78. [[CrossRef](#)]
54. Toth, C.R.A.; Gieg, L.M. Time Course-Dependent Methanogenic Crude Oil Biodegradation: Dynamics of Fumarate Addition Metabolites, Biodegradative Genes, and Microbial Community Composition. *Front. Microbiol.* **2017**, *8*, 2610. [[CrossRef](#)] [[PubMed](#)]
55. Perminova, I.V.; Grechishcheva, N.Y.; Kovalevskii, D.V.; Kudryavtsev, A.V.; Petrosyan, V.S.; Matorin, D.N. Quantification and prediction of the detoxifying properties of humic substances related to their chemical binding to polycyclic aromatic hydrocarbons. *Environ. Sci. Technol.* **2001**, *35*, 3841–3848. [[CrossRef](#)]
56. Qiu, Y.L.; Hanada, S.; Ohashi, A.; Harada, H.; Kamagata, Y.; Sekiguchi, Y. *Syntrophorhabdus aromaticivorans* gen. nov., sp. nov., the first cultured anaerobe capable of degrading phenol to acetate in obligate syntrophic associations with a hydrogenotrophic methanogen. *Appl. Environ. Microbiol.* **2008**, *74*, 2051–2058. [[CrossRef](#)] [[PubMed](#)]
57. Kuever, J. The Family Syntrophorhabdaceae. In *The Prokaryotes*; Springer: Berlin/Heidelberg, Germany, 2014; pp. 301–303.
58. Kleinstuber, S.; Schleinitz, K.M.; Breithfeld, J.; Harms, H.; Richnow, H.H.; Vogt, C. Molecular characterization of bacterial communities mineralizing benzene under sulfate-reducing conditions. *FEMS Microbiol. Ecol.* **2008**, *66*, 143–157. [[CrossRef](#)] [[PubMed](#)]
59. Kunapuli, U.; Lueders, T.; Meckenstock, R.U. The use of stable isotope probing to identify key iron-reducing microorganisms involved in anaerobic benzene degradation. *ISME J.* **2007**, *1*, 643. [[CrossRef](#)]
60. Herrmann, S.; Kleinstuber, S.; Chatzinotas, A.; Kuppardt, S.; Lueders, T.; Richnow, H.-H.; Vogt, C. Functional characterization of an anaerobic benzene-degrading enrichment culture by DNA stable isotope probing. *Environ. Microbiol.* **2010**, *12*, 401–411. [[CrossRef](#)] [[PubMed](#)]
61. Kaplan, I.R.; Galperin, Y.; Alimi, H.; Lee, R.-P.; Lu, S.-T. Patterns of Chemical Changes During Environmental Alteration of Hydrocarbon Fuels. *Ground Water Monit. Remediat.* **1996**, *16*, 113–124. [[CrossRef](#)]
62. Wentzel, A.; Ellingsen, T.E.; Kotlar, H.-K.; Zotchev, S.B.; Throne-Holst, M. Bacterial metabolism of long-chain n-alkanes. *Appl. Microbiol. Biotechnol.* **2007**, *76*, 1209–1221. [[CrossRef](#)] [[PubMed](#)]